ELSEVIER

Journal of Chromatography A, 834 (1999) 433–444

JOURNAL OF CHROMATOGRAPHY A

Applications of capillary electrophoresis in corrosion science and engineering

R.G. Kelly*, J. Yuan, C.M. Weyant, K.S. Lewis

Department of Materials Science and Engineering, Center for Electrochemical Science and Engineering, Thornton Hall, University of Virginia, Charlottesville, VA 22903, USA

Abstract

Four applications of capillary electrophoresis of inorganic ions to the study of corrosion processes are presented. Analyses were conducted of solutions formed on high surface area carbon papers during exposure to corrosive gases, solutions extracted from corroding regions under organic coatings on an aluminum alloy, leachate from chromate conversion coatings on an aluminum alloy, and solutions reconstituted from corrosion products removed from aging aircraft. The flexibility, sensitivity, and robustness of the CE techniques were critical in the analyses required, as was the development of solution extraction methods that were able to retain the important characteristics of the solutions of interest. Analyses for a range of inorganic anions as well as metal cations, including Al^{3+}, Mg^{2+} and Cu^{2+}, are presented.

Keywords: Corrosion; Inorganic anions; Inorganic cations; Organic acids

1. Introduction

The solution chemistry near the metal–solution interface can have a controlling influence on the nature and rate of electrochemical reactions. These reactions often involve the dissolution of the metal. Such corrosion processes are extremely costly, with estimates reaching 4.5% of each country's gross national product. [1] Industrialized nations are thus facing an annual corrosion cost on the order of billions to hundreds of billions of US dollars. In many types of corrosion phenomena, the solution of importance is extremely limited in volume due to physical occlusion or other geometric constraints. Determining the chemical compositions of these occluded solutions is critical to understanding their role in the corrosion process and developing effective mitigation strategies.

Capillary electrophoresis (CE) provides a means to analyze the ionic content of occluded solutions, despite their small volumes. The ionic (as opposed to uncharged, molecular) species are generally regarded as the type that cause corrosion, with anions being particularly important. This paper describes the application of CE as a tool to analyze occluded solutions. Four examples are used to illustrate the process by which CE, when combined with other experimental tools, has been used to improve our understanding of the chemical and electrochemical conditions inside occluded corrosion regions. The four examples are connected via the very limited volumes of solution species available for analysis in each case.

*Corresponding author. Tel.: +1 804 9825783; fax: +1 804 9825799; e-mail: rgkelly@virginia.edu

0021-9673/99/$ – see front matter
PII: S0021-9673(98)01090-5

1.1. Surface active paper (SAP)

Atmospheric corrosion occurs on metals exposed to ambient atmospheres. Although rates are generally low, oxidation rates increase substantially when the relative humidity is above about 60% [2]. Although the extent of metal loss is generally not of concern for structural strength, it can cause failure of electronic circuits, difficulties in soldering of printed circuit boards, and loss of aesthetics, such as in the tarnishing of silver jewelry or serving utensils. The corrosion process occurs more rapidly in the presence of trace amounts (parts per billion by volume) of pollutant gases such as NO_2, H_2S or SO_2. The so-called acid gases are absorbed into the thin water layers that exist on surfaces exposed to air, are hydrolyzed to anions, and lead to corrosion of the metal.

Prevention of atmospheric corrosion is often achieved by the use of protective coatings or volatile corrosion inhibitors (VCI). VCI preferentially absorb onto the metal surface, displacing water. In many applications, these protection schemes are not optimal; connectors on printed circuit boards must be cleaned of the VCI before soldering can be performed. Such cleaning usually involves the use of increasingly-regulated organic solvents. An alternative method of corrosion protection is absorption of the corrosive gas by SAP before the gases can enter the water layer and attack the metal [3]. These papers are cellulose-based, but have large volume fractions of high-surface-area carbon processed into them.

Although the utility of the concept has been demonstrated qualitatively, we have used CE to analyze the capacity of these papers for absorbing different pollutant gases, including the effects of relative humidity on that absorption, and the effect of elevated temperature on subsequent desorption. The occluded solutions of interest in this case are the thin films that form on the SAP surfaces due to adsorption of water and the adsorption–absorption of pollutant gases onto the surfaces or into the water layer. CE results were combined with corrosion rate measurements using the quartz crystal microbalance (QCM) to quantify the efficacy of SAP on reducing atmospheric corrosion of copper exposed to SO_2, NO_2 or H_2S.

1.2. Failure sites in organic coatings

Organic coatings for corrosion protection of metals are used widely due to their ease of application, effectiveness, and low cost. Loss of protection in organic coatings usually occurs at discrete sites rather than catastrophically across the entire surface. These defects can occur due to a range of processes (e.g., chemical or physical heterogeneities) but, in all cases, they contain an aggressive solution that leads to corrosion of the underlying metal. The solutions can develop because of diffusion of water and transport of ionic species through the coating. Historically, only solutions from very large coating defects ($>$10 mm diameter) have been analyzed chemically [4]. To better understand the nature of the solutions that develop and what processes control their development, we have used CE along with microelectrodes to quantify the chemistries within defects that develop in organic coatings on an Al alloy used extensively in the aerospace industry, AA2024-T3. The defects we have studied are in the size range of 1–7 mm in diameter.

1.3. Chromate conversion coatings (CCCs)

Chromate conversion coatings are used widely on Al alloys to prevent corrosion. A chemical process is used to replace the natural Al oxide that is spontaneously forms in air with a much more protective film containing aluminum oxide, chromium(III) oxide, and chromium(VI). Although it has been speculated that the CCCs functioned via leaching of chromate from the film and transport to active corrosion sites, until recently [5] no techniques had sensitivity to determine the leaching of chromate from these thin films. Zhao et al. [5] used Raman spectroscopy to follow the release of chromate from CCCs in 0.1 *M* NaCl solution. We have studied the release of chromate into high-purity water as a simulation of what may happen during exposure to a non-aggressive atmosphere before placement into a corrosive service environment. The ability to leach chromate must be regulated in order to provide long-term protection. CE was used to measure the leaching rates of chromate from CCCs over long-term exposure to small volumes of solution.

1.4. Aging aircraft

Both civilian and military fleets of aircraft are aging. For example, the average age of KC-135 tankers in the US Air Force is over 35 years [6]. Time-dependent processes such as corrosion may limit extension of the service life of such aircraft. One area on aircraft that is particularly vulnerable to corrosion is the lap splice area, the region over which the upper and lower skins are joined to form the fuselage. Water and corrodents can become trapped in the lap splice joint. Corrosion of the skins subsequently occurs and can lead to structural damage. The repair costs for corrosion in these regions are extremely high [7]; the effects on flight safety are currently a matter of much debate.

Understanding the chemical and electrochemical conditions that develop inside these joints is critical to the development of accurate life prediction models. To achieve such understanding, CE has been used to help determine the nature and concentration of the ionic species present in lap joints retrieved from service. Electrochemical testing has been used to determine which of those species impact the corrosion rate of aluminum alloy AA2024-T3, the primary fuselage skin material of most jet aircraft.

2. Experimental

2.1. Corrosion testing methods

2.1.1. SAP

SAPs were obtained from 3M (Minneapolis, MN, USA). One-liter flasks were used as exposure chambers to determine the capacity of the SAP. The flasks were cleaned with Alconox, rinsed, and allowed to dry. A permeation tube, containing the pollutant of interest (i.e., NO_2, SO_2 or H_2S), was placed in the bottom of the flask. Permeation tubes are thick-walled plastic tubes containing a two-phase (gas–liquid) mixture of the pollutant of interest at high pressure. The exposure temperature controls the permeation of the gas through the polymer wall. A 25.8-cm^2 piece of SAP was cut from the supply roll and suspended from a clip embedded in a rubber stopper. The rubber stopper was carefully put in place to seal the flask. Pure air at the selected relative humidity was then purged through the flask for 20 min. The flask was then sealed by pinching of the inlet and outlet tubing of the flask. The flask was then placed in a 30°C water bath where it remained for the duration of the exposure.

2.1.2. Failure sites in organic coatings

AA2024-T3 is an age-hardenable aluminum alloy widely used in jet aircraft for the fuselage skin and other structures. For the organic coating study, the material used had a composition of 4.51 Cu, 1.48 Mg, 0.64 Mn, 0.16 Fe (%, w/w), and remainder Al. The surfaces of the 0.04 in. (1 in.=2.54 cm) thick sheet material were cleaned in Alconox before ultrasonic cleaning in hexane. A vinyl coating was applied via spin coating to a thickness of ~10 μm. After curing, the coated samples were exposed under freely corroding conditions to quiescent 0.6 *M* NaCl or 0.1 *M* KCl for between 14 and 18 days. During this time, blisters in the coated sample due to corrosion processes became visible.

2.1.3. Chromate conversion coatings

Chromate conversion coated AA2024-T3 samples were produced according to published procedures [8]. In addition, samples prepared were obtained from R. Buchheit of Sandia National Laboratory. Both types of samples were immersed in high purity water in sealed containers. Each sample was 17 cm^2 in total surface area, and a total of 8.5 ml of water was added to the container, which was designed in the form of a narrow trough to maximize the surface area-to-volume ratio. Samples were kept at room temperature.

2.1.4. Aging aircraft

A rubber policeman placed on the end of the glass rod was used to scrape corrosion products from lap joints found to have corrosion during routine maintenance of commercial and military aircraft. The corrosion product was collected in a sterile petri dish. Approximately 350 mg of corrosion product was collected on average. The petri dish was taped closed and mailed along with sampling location information to the University of Virginia for analysis.

2.2. Sample extraction and preparation

2.2.1. SAP

In order to extract the adsorbed and absorbed pollutants from the SAP, the flask was removed from the water bath after the specified amount of time had passed. The rubber stopper was carefully removed, to ensure that the SAP did not touch the sides of the flask. The paper was then cut in half and each half was placed into a plastic 50-ml petri dish, which had been previously rinsed with Milli-Q water and dried. Fifteen milliliters of 10 m*M* LiOH was poured into the flask. The paper soaked for 2 days, allowing the pollutant to be desorbed from the paper into the soak solution. This methodology was shown to extract >96% of the species present [9]. After extraction, samples were analyzed along with standards, water, and LiOH blanks. The amount of each ion measured was normalized to the nominal area of the SAP.

2.2.2. Failure sites in organic coatings

Solutions were removed from blisters via the use of a microsyringe pump, as detailed elsewhere [10]. Aliquots between 0.4 and 10 μl were removed, depending upon the size of the blister. The aliquots were then placed in a CE vial, diluted where necessary with high-purity water, and analyzed for their anionic and cationic content.

2.2.3. Chromate conversion coatings

Periodically, aliquots of 100 μl were extracted from the testing solutions for analysis. The volume of solution removed was replaced with high-purity water. The aliquots were analyzed directly, without additional dilution.

2.2.4. Aging aircraft

The main method used for sample extraction was soaking the retrieved corrosion products in 2 ml of high purity water for 24 h. The solution was then removed with a 3-ml syringe. Each solution was passed through a new 0.45-μm filter to remove any insoluble particles before transfer to the capillary electrophoresis vials. Each of four vials was filled with 0.2 ml from a solution sample so that a different vial could be used with each electrolyte. In this way, contamination from carryover could be prevented.

2.3. Analysis procedures

All CE analyses were performed on a Waters Quanta 4000 controlled by Millenium software (version 2.10). The power supply, running mode, lamp and filters used were dictated by the analysis method selected. All water used came from a Millipore UV system. All filters in the water purification system were changed when the concentration of organic acids exceeded 10 μg/l.

2.3.1. Standard and electrolyte preparation

Along with the samples, standards and blanks of high purity water were added to each carousel for CE analysis. The standards used were generated daily by dilution of 1000 mg/l commercial standards or, if unavailable, those prepared from laboratory salts. The commercial standards were Setpoint Laboratory Standards used for ion chromatography and purchased from Analytical Products Group (Belpre, OH, USA). The working standard concentrations ranged from 0.3 to 20 mg/l of each ion.

Four electrolytes were used: chromate and phosphate were used to analyze for anions, while UVCat1 and Modified UVCat2 were used for cations. The electrolytes were prepared using the recipes found in Table 1. OFM-OH is an osmotic flow modifier in the hydroxide form. It was prepared by converting a 20

Table 1
Analysis electrolyte compositions

Electrolyte name	Composition	pH
Chromate	5 m*M* sodium chromate tetrahydrate and 0.5 m*M* OFM-OH	8.0
Phosphate	12.5 m*M* potassium phosphate monobasic, 14.8 m*M* sodium phosphate dibasic, and 1 m*M* OFM-OH, pH adjusted with 0.1 *M* sodium hydroxide	8.0
UVCat1	5 m*M* UVCat1 and 6.5 m*M* HIBA	4.4
Modified UVCat2	1 m*M* UVCat2 (guanidine hydrochloride) pH adjusted with 100 m*M* nitric acid	3.1

m*M* solution of tetradecyl-trimethyl-ammonium bromide (TTAB) by passing it through an anion-exchange resin in the OH^- form from J.T. Baker. One hundred milliliters of electrolyte were prepared at a time and a typical electrolyte was used for 3 weeks. The electrolyte was degassed using a vacuum filtration device.

2.3.2. Capillary preparation

The capillaries used (Polymicro Technologies) were 60 cm long tubes of fused silica with an inner diameter of 75 μm and an effective length (from the sample to the UV window) of 52 cm. A small window (about 2 cm long) of the polymer coating which makes the capillary flexible was removed by burning it with a disposable butane lighter so the UV light could pass through at the detector. After burning, the window was rinsed with methanol. The interior of the capillary was prepared by purging for 2 min with 0.1 *M* KOH. It was then rinsed for 10 min with high-purity water. Finally, the electrolyte was purged through the capillary for 15 min. Each capillary was dedicated to a single electrolyte. After the sample set was completed, the capillary was purged with water for 10 min to prepare for storage.

2.3.3. Instrument parameters

Sample injection was performed hydrostatically for 30 s at a 10-cm elevation. Chromate and phosphate electrolytes were run with a constant current based on the current measured when 17 kV were applied. UVCat1 and Modified UVCat2 were run with a constant voltage of 17 kV. A Hg lamp was used for all analyses, with the appropriate wavelength selected using filters on the lamp and detector. Other parameters are shown in Table 2.

3. Results and discussion

3.1. Capacity testing of surface active papers

Fig. 1 shows electropherograms of soak solutions from SAPs exposed to NO_2. The SAP were exposed to dry (<10% relative humidity, RH) air with an increasing NO_2 concentration (371 μg/l·h) for 192 h at 30°C. The dominant nitrogen species detected in the soak solution was NO_3^-. Fig. 2 shows the relationship between the amount of nitrate detected and the amount of NO_2 permeated. During the test time, the permeation tube was continuously emitting gaseous NO_2. Only after 45 mg of NO_2 has been evolved from the tubes does the amount of NO_3^- detected saturate for the case of adsorption at low RH. At high RH, more NO_2 can be adsorbed onto the papers. This result is likely due to a combination of physical adsorption at both RH on sites that are dry, and absorption of NO_2 into a water layer that forms under the higher RH. Under the higher RH condition used in the present study, the water adsorbed is not a continuous layer, but a series of unconnected islands [11]. Companion studies [12] have shown that the presence of the SAP reduces the corrosion rate of copper exposed to SO_2 at 70% RH by more than an order of magnitude.

The CE studies were also able to show that both the mechanism and the extent of adsorption of pollutant by the SAP vary with the nature of the gas. The solutions extracted from SAP samples that had been exposed to the pollutant gases and then stored in air at either room temperature or heated to 100°C were compared to determine the thermal reversibility of the process for H_2S and NO_2. As shown in Table 3, there is a near complete removal of the NO_2 during heating, whereas there is very little loss in H_2S (detected as sulfate). This difference most likely

Table 2
Instrument parameters

Electrolyte	Current (μA)	Time constant (s)	Power supply	Run time (min)	Detection wavelength (nm)
Chromate	25	0.1	Negative	6	254
Phosphate	50	0.3	Negative	6	185
UVCat1	~5[a]	0.3	Positive	12	185
Modified UVCat2	~10[a]	0.3	Positive	8	185

[a]At a constant voltage of 17 kV.

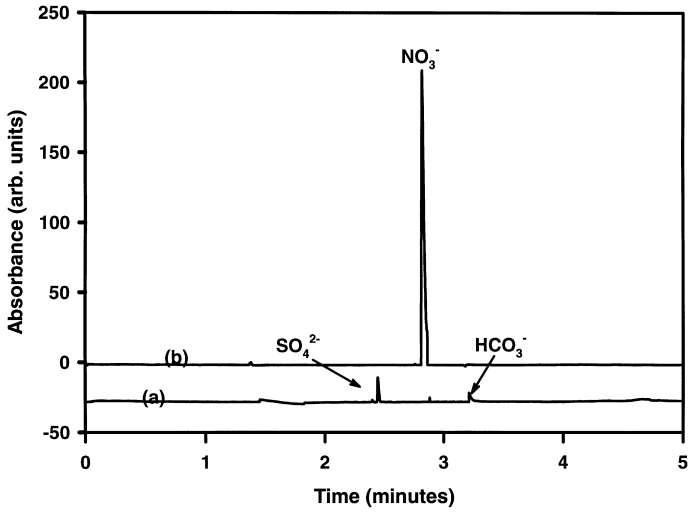

Fig. 1. Electropherograms of solutions removed from surfaces of SAP (a) as-received, (b) exposed to dry (<10% RH) air with an increasing NO_2 concentration (371 μg/l h) for 192 h at 30°C. Chromate working electrolyte used for analysis.

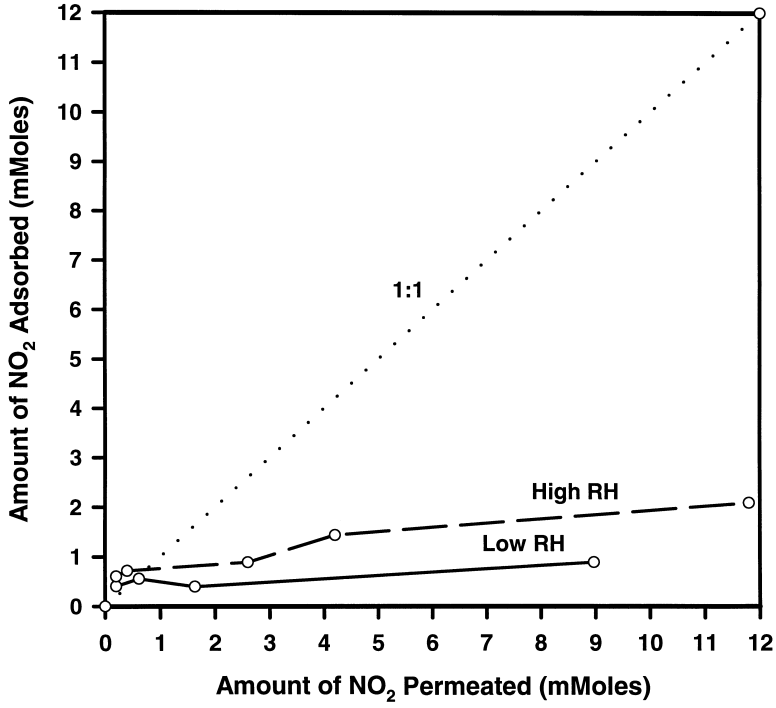

Fig. 2. Capacity results for NO_2 adsorption onto SAP at low humidity at 30°C. The 1:1 line indicates the results expected under conditions for which the SAP capacity exceeds the amount of pollutant permeated. Capacity-limited behavior was observed for both high and low relative humidities. Nominal area of SAP was 25.8 cm^2.

Table 3
Amount of pollutant adsorbed after exposure of SAPs to permeation tubes of different pollutant gases for 48 h and then exposure to air at either room temperature or 100°C for 48 h before extraction

Gas/desorption condition	Amount of pollutant adsorbed (μmol/cm^2)
NO_2/ambient temperature	10
NO_2/heated	0.5
H_2S/ambient temperature	2
H_2S/heated	1.8

results from the irreversible oxidation of H_2S to sulfate upon adsorption to the SAP. The NO_2 either does not react until the soak solution is applied or the reaction is more reversible.

These results have important impact on the utility of the SAP in corrosion prevention. For some gases (like H_2S), temperature variations in the environment will not cause the papers to release the accumulated pollutants. Other gases (like NO_2) could be released when exposed to a thermal fluctuation. Such a situation would allow an accumulation of gases onto the papers at ambient temperature that is then released during exposure to higher temperatures.

3.2. Corrosion conditions inside coating blisters

Exposure of the coated samples to the salt solutions led to the development of small blisters (1–7 mm diameter) within 2 weeks. Fig. 3 demonstrates that there is sufficient sensitivity with CE to analyze solutions from very small blisters (1.5 mm, 100 nl).

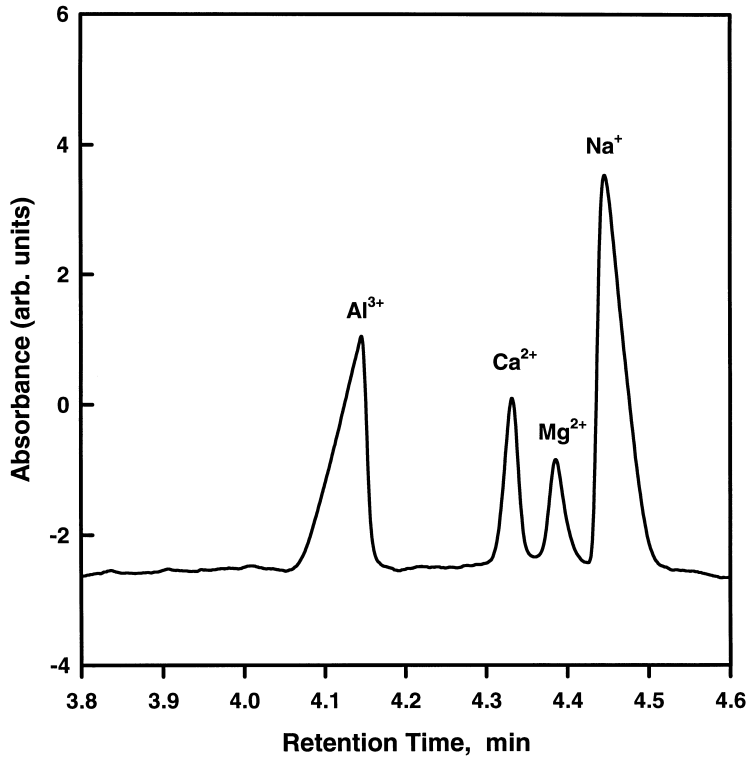

Fig. 3. Electropherogram from 2-mm diameter red blister on vinyl-coated AA2024-T3 after 13 days exposure to 0.6 *M* NaCl. Al^{3+} and Mg^{2+} were dissolved from the alloy, whereas the Na^+ was from the ingress of the bulk electrolyte. The source of the Ca^{2+} was most likely leachant from the organic coating. Modified UVCat2 electrolyte used for analysis.

The anions found originated in the bulk solution or from degradation of the coating itself as a result of the corrosion process. The cations originated from the bulk solution (K^+) and from the dissolution of the alloy substrate (Al^{3+}, Mg^{2+}, Cu^{2+} and Zn^{2+}). Calculations based on the concentrations observed and the known dilutions used showed that a minimum blister size of 500 μm diameter could have its solutions analyzed with CE. These calculations demonstrate that increased sensitivity of the analysis method is not needed as much as an increase in the ability to find and consistently sample from blisters of this size. Typically blisters spend only a short time in that size regime.

The blister chemistry found has been correlated to the intensity of the corrosion activity and the visual appearance of the blister. Actively growing blisters appeared red under optical microscopy and contained substantial concentrations of both anions and cations (see Table 4). In addition, the pH of the occluded solutions in such blisters has been shown to be in the 3–4 range with the use of microelectrodes. Such conditions have been observed in other cases of Al alloy corrosion in which the corrosion site has limited mass transport communication with the bulk solution. The pH observed is controlled by the hydrolysis of aluminum ions [13,14].

In some cases, active blisters will cease to grow and turn black in appearance. These blisters contain much lower concentrations of all ions and a near neutral pH. The minimum solubility of $Al(OH)_3$ occurs at pH 5.2. Thus, if the acidic conditions necessary for active dissolution cannot be maintained, then the precipitation of hydroxide will occur and will tend to control the pH, although the presence of other species may also have an impact.

Clear blisters have also been observed in which very little corrosion occurs, but a delamination of the coating from the substrate is detectable. These blisters have very low concentrations of ions and a mildly alkaline pH. These blisters are likely the location of the cathodic reactions that support the actively growing blisters. Both of the common cathodic reactions in aqueous corrosion (oxygen and water reduction) lead to an increase in the local pH.

The observation of organic acids in some blisters corresponds to attack of organic coating itself by solution formed in blisters. These results are potentially of great importance in determining the contributions of various mechanisms by which blisters in organic coatings on metals grow. If the interface between the coating and the metal is susceptible to attack on the coating side, then organic acids will be produced. Undercutting of the coating by dissolution of the metal can also occur. Determination of the relative contributions of these paths will be part of future work in this area in order to provide information for the design of better protective coating systems.

The CE analyses in this work are critical not only for better understanding the mechanisms controlling the formation and growth of coating system defects, but also for the development of life-prediction models for coatings. Such models require chemical and electrochemical boundary conditions. The CE analyses can provide the chemical boundary conditions. In addition, bulk analogues of the occluded solutions can be made and the chemical and electro-

Table 4
CE results for the pinhole samples in 0.1 *M* KCl

Color	Solution sampled (nl)	Al^{3+} (mg/l)	Mg^{2+} (mg/l)	Mn^{2+} (mg/l)	Cu^{2+} (mg/l)	K^+ (mg/l)	Cl^- (mg/l)	Formate (mg/l)	Acetate (mg/l)
Clear	600	DL	DL	DL	DL	5844	176	DL	QL
Clear	1800	DL	DL	DL	DL	5881	487	DL	800
Red	5900	2034	167	76	668	1464	16 465	DL	DL
Red	10 700	851	206	69	32	2318	12 534	710	338
Black	400	DL	10	QL	QL	268	157	DL	DL
Black	400	DL	DL	DL	DL	3833	1587	DL	DL

DL, below minimum detection limit; QL, below minimum quantification limit.

chemical behavior of the substrate and organic coating can be determined. These are also focuses of future work.

3.3. Chromate leaching from chromate conversion coatings

Fig. 4 shows a progression of electropherograms collected from aliquots removed during the leaching tests. The increase in the chromate signal is clear over the 1548 h. An increase in the chloride signal is also observed. The water used was checked, as was a blank, indicating that the source of the chloride was the CCC. Small peaks due to formate and acetate were also observed, but these did not change with time and were likely due to contamination from the container. Fig. 5 shows the time course of the total amount of chromate leached from both a laboratory-prepared CCC and a commercially-prepared CCC. The two preparations show very similar leaching rates. These rates are far lower than those observed by Zhao et al. in 0.1 *M* NaCl [5]. With similar surface area to volume ratios, they observed leaching rates decrease from 2 mg/l h for 20 min aging to 0.38 mg/l h for 10 day-old coatings. Our results indicate a rate of 10^{-4} mg/l h. Taken together, these results indicate the presence of a mechanism that allows retention of the chromate in an insoluble form under non-corrosive conditions (high purity water), but then allows its release upon exposure to more corrosive conditions (0.1 *M* NaCl). The high sensitivity of CE allowed the measurement of the very slow leaching of chromate in distilled water.

3.4. Corrosion chemistry inside aircraft lap joints

Corrosion chemistries of lap joint solutions were found to be exceedingly complex with up to 22 different ionic species detected [15]. Fig. 6 shows an electropherogram from a chromate analysis of a lap joint corrosion product showing an example of the wide variety of anions detected. Identification of

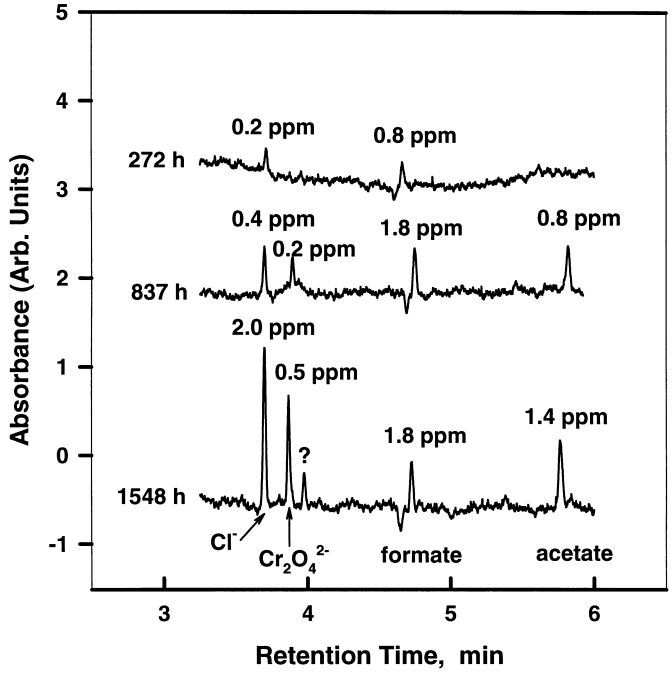

Fig. 4. Time series of electropherograms from leaching of chromate from chromate conversion coated AA2024-T3 in high purity water. Organic acids were most likely from contamination of cell, whereas the chromate and chloride appear to be from the conversion coating. Phosphate electrolyte used for analysis (ppm stands for mg/l).

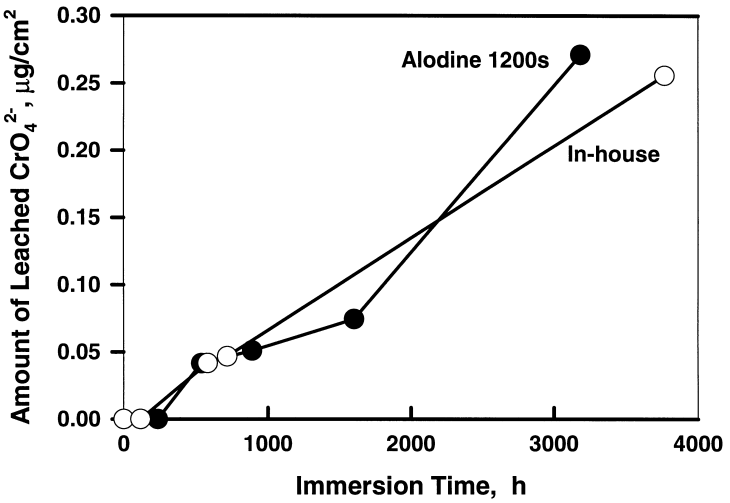

Fig. 5. Amount of chromate leached from two chromate conversion coated samples over long times, showing quantitatively similar behavior for (●) commercially prepared and (○) laboratory-prepared coatings.

each species was accomplished by spiking. The most commonly found anions were chloride, sulfate, nitrate and bicarbonate. Aluminum, potassium, sodium and magnesium were commonly found cations. Commonly found ions were defined as those present in at least 75% of the 60 sample solutions studied which were extracted from eight aircraft. Also detected less frequently were nitrite, fluoride, phosphate, acetate, chloroacetate, propionate, formate, lactate, butyrate, calcium, manganese, zinc, strontium and copper.

Electrochemical testing showed that very few of the ionic species detected had a statistically significant effect on measured corrosion parameters [15]. The anions shown to have a statistically significant effect on the corrosion behavior of AA2024-T3 are

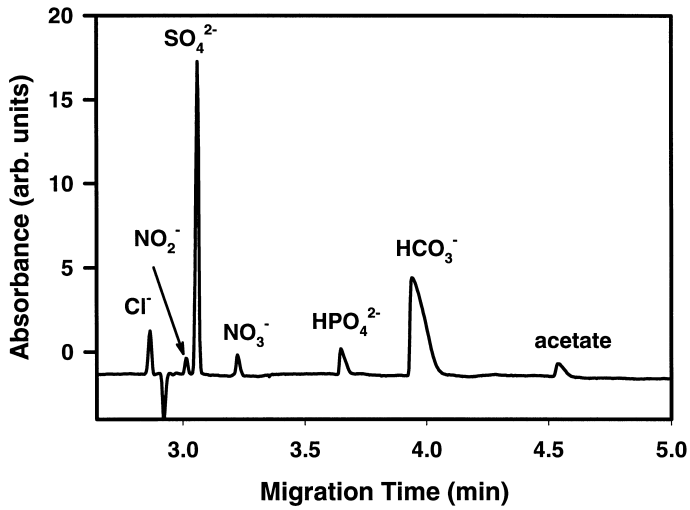

Fig. 6. Electropherogram of extraction solution from corrosion products formed in occluded region of an aircraft fuselage. Chromate electrolyte was used for analysis.

Table 5
Maximum concentrations of ions and the frequency with which they were found in reconstituted lap splice joint solutions from in service aircraft

Ion	mg/l	m*M*	Frequency (%)
Chloride	**687.4**	**19.363**	75
Nitrate	**190.5**	**4.141**	63
Nitrate	100.8	1.626	95
Sulfate	208.8	**2.131**	86
Hydrogen bicarbonate	**399.4**	**6.548**	83
Formate	530.2	11.782	46
Acetate	124.1	2.103	78
Phosphate	232.7	2.449	46
Fluoride	**76.3**	**4.016**	32
Propionate	301.1	4.125	47
Butyrate	96.6	1.110	35
Oxalate	0.6	0.007	<5
Phthalate	191.4	1.338	<5
Benzoate	0.4	0.004	<5
Chloroacetate	2.9	0.031	5
Sodium	1618.6	70.374	78
Potassium	935.2	23.979	85
Aluminium	50.5	1.870	79
Strontium	4.6	0.053	<5
Calcium	881.2	22.030	25
Copper	102.4	1.613	13
Magnesium	2121.1	88.379	81
Manganese	9.9	0.180	<5
Zinc	1.0	0.015	<5
Barium	101.5	0.741	<5
Lithium	101.0	14.429	<5

Bold indicates ions that were shown to have a statistically significant effect on the corrosion behavior of AA2024-T3.

indicated in Table 5 by the bold typeface. This result is critical in that it allowed a solution composition to be specified that was not extremely complex, but nevertheless reproduced the nature of the corrosion observed in actual field conditions. This solution composition is now being used in several laboratories as a simulant for lap splice conditions in testing of fatigue crack growth, localized corrosion susceptibility, thinning rate, and corrosion prevention compound efficacy.

4. Conclusion

The four cases presented provide a range of examples in which the ability of CE to measure the ionic composition of occluded solutions of importance in corrosion and its prevention was critical. Sample extraction required the consideration of maintenance of the chemistry of the solution. The flexibility of CE allowed these solutions of small volume to be fully analyzed for their composition which allowed insights into the mechanisms controlling corrosion to be better elucidated.

Acknowledgements

The authors would like to acknowledge the financial support of AFOSR (Grant F49620-96-1-0178, Maj. H. DeLong), 3M (C. Markell), and NASA (Langley Research Center—R. Piascik). Equipment support from Waters Corporation is also gratefully acknowledged. The chromate conversion coatings were prepared by Dr G.O. Ilevbare (University of Virginia).

References

[1] Economic Effects of Metallic Corrosion in the United States, Report by Batelle Laboratories, Columbus, OH, 1995.
[2] D. Fyffe, in: L.L. Shreir (Ed.), Corrosion, vol. 1, ch. 2.2, Butterworths, London, 1979.
[3] 3M Product Bulletin, Model 2102 Corrosion Control Adsorber Patches, 3M Electrical Specialties Division, Austin, TX, 1993.
[4] S. Haruyama, M. Asari, T. Tsuru, in: M.W. Kendig, H. Leidheiser (Eds.), Proceedings of the Symposium on Corrosion Protection by Organic Coatings, PV 87-2, Electrochemical Society, Pennington, NJ, 1987, p. 11.
[5] J. Zhao, G. Frankel, R.L. McCreery, J. Electrochem. Soc. 145 (1998) 2258.
[6] D. Groner, D. Neiser, Can. Aeronautics Space J. 42(2) (1996) 63.
[7] R. Kinzie, G. Cooke, in: Proceedings of the 2nd Joint NASA/FAA/DoD Conference on Aging Aircraft, Williamsburg, VA, 31 Aug.–3 Sept. 1998 (in press).
[8] ASM Handbook, 10th ed., vol. 5, ASM International, OH, 1994, p. 482.
[9] J. LaScala, Senior Thesis, School of Engineering and Applied Science, University of Virginia, Charlottesville, VA, 1997.
[10] K.S. Lewis, J. Yuan, R.G. Kelly, J. Chromatogr. (submitted for publication).
[11] N.D. Tomashov, Theory of Corrosion and Protection of Metals, Macmillan, New York, 1966.

[12] C.M. Weyant, M.S. Thesis, School of Engineering and Applied Science, University of Virginia, Charlottesville, VA, 1998.
[13] A. Turnbull, Corros. Sci. 23 (1983) 833.
[14] C.F. Baeses, R.E. Mesmer, The Hydrolysis of Cations, Wiley, New York, 1976.
[15] K.S. Lewis, S. Willard, R.S. Piascik, R.G. Kelly, Determination of the corrosion conditions within aircraft lap-splice joints, in: Proceedings of the 2nd Joint NASA/FAA/DoD Conference on Aging Aircraft, Williamsburg, VA, 31 Aug.–3 Sept. 1998 (in press).